

# Supporting Information

Bonneaud et al. 10.1073/pnas.1018580108

## SI Materials and Methods

**Capture, Housing, and Experimental Infection.** Birds were captured at the two sites using mist nets or wire mesh cages placed around feeders. Following capture, birds were immediately transported by plane from Arizona ( $n = 37$ ) and by car within Alabama ( $n = 64$ ) and established in aviaries at Auburn University, Auburn, Alabama. Birds were housed in cages as pairs for the duration of their period in captivity. Cages were kept indoors in temperature-controlled rooms with windows, and birds were fed sunflower seed, brown and white millet, and water ad libitum, as well as apple slices and crushed eggshells on a weekly basis. Grit was provided to allow digestion of seeds. Birds from Alabama and Arizona were kept in separate rooms for the first month to check that birds were MG-free. Following quarantine, birds were measured and blood was sampled using brachial venipuncture ( $\sim 60$   $\mu$ L of whole blood) and examined for exposure to *Mycoplasma galliseptum* (MG) using serum plate agglutination assay (1) and amplification of MG DNA from choanal and conjunctival swabs (2). No birds used in any part of the experiment were found to have been previously infected with MG. Twelve birds from the Alabama population were removed from the experiment following evidence of exposure to MG (8 were symptomatic at capture, 1 developed symptoms during quarantine, and 3 were seropositive for MG antibodies), and 15 from Arizona and 32 from Alabama were used in a different experiment, leaving 22 Arizona birds and 21 Alabama birds in this study.

Birds were kept either as controls or infected via ocular inoculation with 20  $\mu$ L of culture containing  $1 \times 10^4$  to  $1 \times 10^6$  color-changing units/mL of an early 2007 Auburn MG isolate (BUA #243). Control birds were sham-infected using sterile SP4 medium (3). Control and infected birds were maintained under identical conditions, but in separate rooms of the aviary. After exposure, birds were monitored daily for disease onset and progression of symptoms. All experimentally infected birds tested positive for MG DNA in their choanal cleft at 3 and 14 d postinfection, and all were seropositive after 2 wk. All control birds remained negative for MG DNA and for MG antibody agglutination throughout the course of the experiment. Fourteen days postinfection, birds were euthanized under license. The spleens and the eyes/conjunctivae from all euthanized birds were immediately removed, stored in RNAlater (Ambion), and placed at  $-80$   $^{\circ}$ C.

**Quantification of MG Using TaqMan Quantitative RT-PCR Assays.** We randomly selected one eye with conjunctivae from each bird 14 d after infection. We isolated total genomic DNA from both MG and house finches using the Qiagen AllPrep DNA/RNA Mini Kit. MG quantification was then performed as described (4) by running quantitative RT-PCR (qRT-PCR) assays on the *mgc2* gene. We also amplified the house finch *rag1* gene to control for variation in amounts of starting material. Reactions were run on an ABI Prism 7500 (Applied Biosystems). We made a standard curve for both genes using 100, 50, 25, 10, 1, and 0.1 g/L of genomic DNA to estimate the relative amount of MG between individuals. Each reaction consisted of 25  $\mu$ L of TaqMan PCR Master Mix (2), No AmpErase UNG (Applied Biosystems), 0.45  $\mu$ L each of 100  $\mu$ M forward and reverse primers, 1.25  $\mu$ L of 10  $\mu$ M probe, 17.85  $\mu$ L of DNase-free water, and 5  $\mu$ L of 10 g/L sample. Cycling parameters were 50  $^{\circ}$ C for 2 min, 95  $^{\circ}$ C for 10 min, followed by 50 cycles for 95  $^{\circ}$ C for 15 s and 60  $^{\circ}$ C for 1 min. We used the automatic threshold settings for analysis of our samples.

**Microarray Construction, Hybridization, and Analysis. Microarray construction.** We constructed a microarray using cDNA clones from the subtraction suppression hybridization (SSH) libraries constructed in Wang et al. (5) and enriched in cDNA differentially expressed between MG-infected and control house finches 2 wk postinfection. The microarray consisted of 1,000 unique amplicons and included the 220 clones previously identified as significantly differentially expressed between control and infected house finches using a macroarray approach (5), as well as 694 randomly selected clones from the libraries, many of whose expression responses to infection are unknown (5). The clones were collected from the SSH libraries with a toothpick and grown in 1.3 mL of LB + ampicillin at 37  $^{\circ}$ C overnight. We isolated the plasmid DNA using a Plasmid and BAC extraction kit (AutoGen) on an AutoGenprep 965. We amplified 5  $\mu$ L of the eluted DNA in 10  $\mu$ L buffer 10 (Lucigen), 0.8  $\mu$ L dNTP (100  $\mu$ M), 8  $\mu$ L of each primer M13/M13R (10  $\mu$ M), 0.8  $\mu$ L (4 U) EconoTaq DNA polymerase (Lucigen), and 56.4  $\mu$ L of sterile dH<sub>2</sub>O. The reaction was run for 35 cycles consisting of a 90-s at 94  $^{\circ}$ C denaturing step, a 45-s at 50  $^{\circ}$ C annealing step, and a 45-s at 72  $^{\circ}$ C extension step. PCR products were purified using a QIAGEN MinElute 96 UF purification kit and run on a 2% agarose gel. Amplified inserts were subsequently printed onto the array slides.

We also printed five house finch “housekeeping” genes to help in normalization procedures (*actin-related protein 2/3*, *ATP synthetase*, *ATPase VI subunit G1*, *basic transcription factor 3*, and *calmodulin 2*). These genes were generated by amplification of cDNA extracted from house finch spleens (see below), using degenerate primers designed from conserved sequences of humans, mice, chicken, and, when available, zebra finches. We amplified 2  $\mu$ L of cDNA in 2.5  $\mu$ L buffer 10 (Lucigen), 2.5  $\mu$ L dNTP (100  $\mu$ M), 1  $\mu$ L of each primer (10  $\mu$ M), 0.2  $\mu$ L (2.5U) EconoTaq DNA polymerase (Lucigen), and 15.8  $\mu$ L of sterile dH<sub>2</sub>O. The reaction was run for 35 cycles consisting of a 1-min at 94  $^{\circ}$ C denaturing step, a 2-min at 60  $^{\circ}$ C annealing step, and a 3-min at 72  $^{\circ}$ C extension step. PCR products were run on a 2% agarose gel and purified using a QIAGEN MinElute 96 UF purification kit. Each gene was amplified twice and although we kept one reaction intact, we ligated and transformed the other into One Shot TOP10 Chemically Competent *Escherichia coli* using the TOPO cloning kit (Invitrogen). Colonies were picked and added to 1.3 mL of LB medium with ampicillin to grow overnight at 37  $^{\circ}$ C. We then isolated the plasmid DNA using a plasmid and BAC extraction kit (AutoGen) on an AutoGenprep 965. We amplified 2  $\mu$ L of the extracted plasmids in 2.5  $\mu$ L buffer 10 (Lucigen), 0.2  $\mu$ L dNTP (100  $\mu$ M), 2  $\mu$ L of each primer M13/M13R (10  $\mu$ M), 0.2  $\mu$ L (2.5 U) EconoTaq DNA polymerase (Lucigen), and 14.1  $\mu$ L of sterile dH<sub>2</sub>O. All PCR products were purified using a QIAGEN MinElute 96 UF purification kit and run on a 2% agarose gel. We verified the identity of the purified PCR products by sequencing them on an ABI 377 DNA sequencer (see below). We printed both the PCR products and the transformed PCR products of the five house finch housekeeping genes onto the array slides. We quantified purified PCR products on a Nanodrop spectrophotometer.

Additionally, we printed the PCR products from the DNA amplification of 11 *E. coli* housekeeping genes (*arcA*, *aroE*, *dnaE*, *gapA*, *gnd*, *icdA*, *pgm*, *polB*, *putin*, *trpA*, and *trpB*) to serve as external spike-ins (6). DNA was extracted from a few *E. coli* colonies obtained above using the QIAGEN DNeasy tissue, and we amplified *E. coli* housekeeping genes as described (7, 8).

PCR products were purified, sequenced, and quantified as described above.

We printed the clones on poly-L-lysine-coated glass slides using an OmniGrid 100 (GeneMachines, BST Scientific). All clones were printed twice on each half grid, and each grid was replicated twice on each microarray slide. After printing, the slides were blocked by rehydration and UV crosslinking at 60 mJ and dipped in blocking solution (6 g succinic anhydride, 335 mL 1-methyl-2-pyrrolidinone, 15 mL sodium borate). Denaturing was subsequently performed by dipping the slides in MiliQ water and then in 95% ethanol and spun dry by centrifugation for 2 min at 1,000 × g. The desiccated slides were stored at room temperature in a closed container until further use.

**Sample preparation and microarray hybridization.** The slides were hybridized with the samples collected from the experimental infections. We extracted total RNA from ~17 mg of sonicated spleen tissue using Qiagen RNeasy miniprep spin columns followed by DNase digestion of genomic DNA according to the manufacturers' protocols. Gene expression changes were examined in the spleen because this tissue plays an important role in the organization of both the innate and the acquired immune responses in humans as well as in birds, in addition to its role of filtering blood and removing old erythrocytes (9, 10). Indeed, asplenic human infants are found to be extremely sensitive to bacterial infections, and the lack of a spleen results in defective Th cells, decreased antibody responses, and a lack of important macrophages (11, 12). We determined the quantity of purified total RNA using a Nanodrop spectrophotometer and determined RNA integrity on an Agilent 2100 Bioanalyzer. All RNA extracts were stored at -80 °C until further processing.

We pooled two to five spleens from birds from the same population in the same treatment to generate enough mRNA for microarray hybridizations. We had two pools of mRNA for each treatment from each population. mRNA pools were labeled using Cy5 dye and were then hybridized against a common reference, made by pooling an aliquot of all of the individual samples and labeling with Cy3. We made a calibration curve of hybridization efficiency by diluting the *E. coli* external PCR products at known concentrations. Each hybridization was performed on one half-slide. Each pooled house finch RNA sample was prepared for cDNA microarray hybridization by reverse-transcribing 15 µg of total pooled RNA in 30.8-µL reaction volumes containing 1 µL of a mix of oligo(dT) (dT12-, 13-, 14-, 15-, 16-, 17-, and 18-mer; final concentration: 5 µg/µL), 6 µL of 5 First Strand Buffer (Invitrogen), 3 µL of 0.1 M DTT, 0.8 µL 50 aminoallyl-dUTP/dNTP mix (20 mM dATP, 20 mM dCTP, 20 mM dGTP, 12 mM dTTP, 8 mM aminoallyl-dUTP), 2.5 µL (500 U) of SuperScript II Reverse Transcriptase (Invitrogen). Reactions were incubated at 42 °C for 3 h. cDNA samples were subsequently hydrolyzed by adding 10 µL of 1 M NaOH and 10 µL of 0.5 M EDTA and incubated at 65 °C for 15 min. Neutralization was performed by addition of 25 µL 1 M Hepes (pH 7.5).

We prepared the external spike-ins by dividing the product from each *E. coli* gene amplification into two. We incorporated the aminoallyl dUTP by adding 24 µL of nuclease-free H<sub>2</sub>O to 1 µg of each sample. We also added 20 µL of BioPrime 2.5 random primer mix (Invitrogen) and boiled the reaction for 5 min before incorporating 5 µL of 10 aminoallyl-dUTP/dNTP mix (4.8 mM dATP, 4.8 mM dCTP, 4.8 mM dGTP, 1.6 mM dTTP, 3.2 mM aminoallyl-dUTP) and 1 µL (40–50 U) of Klenow fragment to each tube. We incubated the mixture at 37 °C for 2 h and stopped the reaction with 5 µL 0.5 M EDTA. For each *E. coli* gene, the labeled samples were serially diluted, and we added pools of the more concentrated products to the common house finch reference (final concentrations: *polB* and *dnaE* at 182 pg/µL, *trpA* and *putin* at 91 pg/µL, *pgm* and *arcA* at 18.2 pg/µL, *gnd* and *gapA* at 3.64 pg/µL, *trpB* and *icdA* at 1.82 pg/µL), and a pool of diluted products to each of the house finch-labeled cDNA samples (all

samples added at a final concentration of 1.82 pg/µL) to obtain final concentration ratios of 1:1, 1:2, 1:10, 1:50, and 1:100.

We purified the mixtures using microcon-30 filters. We added 1 µL of NaHCO<sub>3</sub> to 10 µL purified probe. We resuspended the cyanine dyes (Cy3 and Cy5) with the probe and incubated the mixture in the dark at room temperature for 2 h to allow coupling of the cDNA to the *N*-hydroxy succinamide ester of the dyes. All samples were labeled using Cy5 dye, and the common reference was labeled with Cy3. The mixtures were then purified using the QIAGEN QIAquick PCR purification kit. The eluted Cy3- and Cy5-labeled probes were combined and added into a microcon-30 filter and spun for 3 min at 10,000 × g; the filter was then inverted and spun at 4,500 × g for 5 min. We prepared the concentrated probes for hybridization by adding 3 µL of 20 SSC, 1.5 µL poly(A) (7 µg/µL), and 0.48 µL 1 M Hepes (pH 7.0), and we applied the mixture to prehumidified Millipore 0.45-µm filters, spun them at 10,000 × g for 1 min, and stored the flow-through at 4 °C until further use.

Immediately before hybridization, we added 0.45 µL 10% SDS to the probe, heated it for 2 min at 100 °C, and allowed it to cool down at room temperature for 10 min. The arrays were placed in Corning microarray hybridization chambers and a clean Lifter-slip (Eerie Scientific) was placed over each array. After injecting the probes under the Lifterslips, we added 50 µL of SSC to the hybridization chambers and placed them in a 62 °C water bath for 12–16 h. Following hybridization, the slides were washed in 0.2 SSC with 2% SDS and then in 0.2 SSC. We spun the slides dry by centrifuging them at 1,000 × g for 2 min and scanned using an Axon 4000A microarray scanner (Axon Instruments).

**Statistical analysis of microarray data.** We used the software package GenePix to yield log base-2 (log<sub>2</sub>) measurements for mean fluorescence intensities for each dye channel in each spot on the array and to flag low-quality spots. Normalization of the raw fluorescence intensities was performed in three steps using a Bioconductor package *marray* and *limma* (13) implemented in R language (<http://www.r-project.org>). First, background adjustment was performed using the *normexp* method. Second, spatial and print-tip loess normalization (2D method) were performed to remove spatial and dye biases for each slide. Third, we performed a scale normalization to control for variation between slides.

The ratios generated by the external spike-ins were used for quality control. To control for within-hybridization spatial variation, we compared the signal from the two replicated grids. To control for between-slide differences, we compared the signals from the *E. coli* external spike-ins, the house finch housekeeping genes, and the common reference on the different slides. All clones were printed twice on each array and were considered to be differentially expressed only when both replicates displayed a significant deviation from the mean of the standard.

To determine gene expression differences between samples, normalized log<sub>2</sub> transformed signal ratios (sample vs. reference) were fitted to a general linear model with two factors representing treatment (control and infected) and population of origin (MG-exposed Alabama and MG-unexposed Arizona) and using the equation:

$$Y_{ijc} = \mu + A_i + B_j + AB_{ij} + \varepsilon_{ijc},$$

where  $Y_{ijc}$  is the log<sub>2</sub> measurement for a particular clone ( $c$ ) from a particular treatment ( $i$ ) and a particular population of origin ( $j$ ),  $\mu$  is the parametric mean,  $A$  and  $B$  correspond to the single-factor effects (treatment and population of origin, respectively),  $AB$  is the two-way interaction between the two main effects, and  $\varepsilon$  is the residual between the data and the model.

We identified clones that were significantly differentially expressed between the following groups: (*i*) infected vs. controls in Arizona; (*ii*) infected vs. controls in Alabama; (*iii*) control birds from Arizona vs. control birds from Alabama; and (*iv*) infected

birds from Arizona vs. infected birds from Alabama. These comparisons allowed us to evaluate changes in gene expression between treatments within geographic populations, as well as within treatments between populations.

**Sequencing and Gene Ontology analyses.** All of the 162 clones found to be significantly differentially expressed between groups were subsequently sequenced. We added 1  $\mu\text{L}$  of Big Dye (Applied Biosystems), 2  $\mu\text{L}$  of buffer 5 and 2  $\mu\text{L}$  of primer M13 or M13R (1  $\mu\text{M}$ ) to 5  $\mu\text{L}$  of PCR product. The reaction was run for 30 cycles consisting of 10 s at 94  $^{\circ}\text{C}$ , 5 s at 50  $^{\circ}\text{C}$ , and 4 min at 60  $^{\circ}\text{C}$  and a final extension of 1 min at 60  $^{\circ}\text{C}$ . The sequencing reaction cleanup was performed by adding 2.5  $\mu\text{L}$  of 125 mM EDTA to each reaction and 25  $\mu\text{L}$  95–100% ethanol and then incubating this solution for 15 min at room temperature and centrifuging at  $3,000 \times g$  for 30 min. The tubes were then inverted and centrifuged at  $190 \times g$ , and we added 30  $\mu\text{L}$  of 70% ethanol, centrifuged for 15 min at  $1,650 \times g$ , and then inverted and spun at  $190 \times g$  for 1 min. The cleansed sequence reaction pellet was resuspended with 10  $\mu\text{L}$  of HiDi-Formamide before sequencing on an ABI 377 sequencer. Forward and reverse sequences generating a BLAST hit with an  $e$ -value  $< 1 \times 10^{-20}$  with more than 100 nucleotides were categorized by their vertebrate homologs, and all other genes were considered to be unknown. Gene ontology category and function were determined using Harvester (<http://harvester.fzk.de/harvester/>).

#### Microarray Validation Using Multiplex Quantitative RT-PCR Analysis.

We verified transcriptional changes at 16 genes using multiplex quantitative real-time amplifications (qRT-PCR) (14). Multiplex qRT-PCRs require only a small amount of RNA to simultaneously assess individual variation in expression of up to 30 different genes per sample. Genes were selected if they were significantly differentially expressed in the microarray experiment and if they were of known, particularly immune-related, Gene Ontology (GO) functions (*Ig J*, *parathymosin*, *MHC class II-associated invariant chain Ii*, *Ig superfamily member 4A isoform a*, *TCR  $\beta$ -chain*, *hsp90*, *NADH dehydrogenase subunit 4*, *thioredoxin*, *prosaposin*, *eukaryotic translation initiation factor eIF4E*, *nucleic acid binding protein RY-1 variant 3*, *MAK-like kinase*, *RhoA GTPase*, *ubiquitin C*, *lymphocyte cytosolic protein*, and *SEC61  $\gamma$ -subunit*) for inclusion in a single multiplex. We also included two house finch housekeeping genes (*actin-related protein 2/3* and *calmodulin 2*) that were used in the microarray experiment to help in the normalization of qRT-PCR results.

Primers were designed using GeXP Express Profiler Primer Design software (Beckman). Each primer pair was designed to yield PCR products at least 7 bp apart (ranging from 139 to 341 bp) with similar GC content and melting temperature. We also included primers to amplify a kanamycin RNA transcript that was spiked into each reaction as an external control (GenomeLab GeXP Start Kit; Beckman Coulter). Multiplex qRT-PCR maintains relative transcript abundances through incorporation of universal tags that are homologous to the 5' ends of the forward and reverse primers. The forward universal primer carries a fluorescent dye label so that, following amplification, the PCR products can be examined by capillary electrophoresis (Beckman Coulter CEQ8000) for fragment size determination.

Two contrasting analytical approaches were used to validate microarray data. First, we used a correlational approach to determine whether the degree to which genes are differentially expressed in the microarray is related to the degree to which they are differentially expressed in a multiplex qRT-PCR. Differential expression of genes in the microarray is defined as that in which the expression of the same gene differs significantly either between treatments within the same population or between populations within treatments. As predicted, a Spearman's rank correlation showed a significant positive relationship between the ranks of expression from the microarray and the multiplex qRT-

PCR data ( $r_s = 0.46$ ,  $n = 45$ ,  $P < 0.001$ ). Second, we used a one-sampling  $t$ -test framework to determine whether up-regulation of expression in the microarray is associated with up-regulation using qRT-PCR and vice versa. Two analyses were conducted using the following comparisons: (i) control birds from Arizona vs. Alabama ( $n = 11$  genes) and (ii) infected birds from Arizona vs. Alabama ( $n = 16$ ). In both analyses, up-regulation in the microarray was associated with up-regulation in the multiplex qRT-PCR (and vice versa): (i)  $T_{10} = 2.26$ ,  $P = 0.024$  and (ii)  $T_{15} = 3.33$ ,  $P = 0.002$ . ( $P$  values represent one-tailed estimates because in all cases the microarray is upheld only if the qRT-PCR results are greater than zero.)

**Statistical Analyses.** The validity of all further analyses was confirmed using Zar (15).

**Microarray validation.** A Spearman's rank correlation was conducted because neither the microarray nor the multiplex qRT-PCR values were normally distributed [Shapiro–Wilk test for normality:  $W = 0.93$ ,  $n = 44$ ,  $P = 0.007$  (microarray);  $W = 0.68$ ,  $n = 44$ ,  $P < 0.001$  (qRT-PCR)].  $t$ -Tests were conducted because interpopulation differences in gene expression between control and infected populations did not differ from normality [Shapiro–Wilk test for normality:  $W = 0.95$ ,  $n = 11$ ,  $P = 0.69$  (microarray);  $W = 0.91$ ,  $n = 16$ ,  $P = 0.12$  (qRT-PCR)].

**Interpopulation/treatment comparisons.** Intero-population/treatment comparisons (Fig. 2A) were analyzed using two-tailed binomial tests, Fisher exact tests, or goodness-of-fit tests. Two-tailed binomial tests resemble  $2 \times 2$   $\chi^2$  contingency tables and give qualitatively similar results except that they are more appropriate when comparing between two proportions. Fisher exact tests were used when sample sizes were such that expected values failed to reach 5. Goodness-of-fit tests were used to compare whether an observed frequency differed from the expected.

**MG analyses.** Population differences in MG were analyzed using a general linear model with normal error structure in which MG load was fitted as the response term, amount of host tissue was fitted as a covariate, and population was fitted as the main term of interest. The distribution of MG loads did not differ significantly from normality (Shapiro–Wilk test for normality:  $W = 0.97$ ,  $P = 0.74$ ) and the variance in MG load between populations did not differ significantly (Bartlett's test for homogeneity of variance:  $\chi_1^2 = 0.00$ ,  $P = 0.96$ ). The relationship between MG load and expression levels was conducted using a linear regression. MG load was expressed as a ratio of host tissue and used as the response term in the analysis. The distribution of MG load ratio did not differ from normality (Shapiro–Wilk test:  $W = 0.94$ ,  $P = 0.22$ ).

**Online Gene Functions.** Among the known genes that were significantly differentially expressed (Table S1), we identified 10 with primary immune function, which hence could be directly involved in the immune response to MG. For example, of the 6 genes differentially expressed in comparisons 1 and 2 (Fig. 2A and B), MHC class II-associated invariant chain Ii plays a role in the assembly of MHC class II molecules, which serve to recognize foreign peptides originating from the degradation of extracellular parasites (16); lectin galactoside-binding soluble 2 protein (galectin 2) belongs to a family of proteins differentially expressed in various immune cells and up-regulated during infections (17); galectins are involved in the regulation of cellular immune responses and immune cell homeostasis (18), and galectin 2 is thought to control inflammation and regulate activated CD8+ T cells (19); programmed death ligand 1 plays a key role in regulating T-cell activation and tolerance (20, 21); neutrophil cytosolic factor 4 (40 kDa) encodes for a subunit of the superoxide-producing phagocyte NADPH oxidase and plays an important role in phagocytosis-induced superoxide production, an essential mechanism in host innate immune defense (22); T-cell

immunoglobulin and mucin domain containing 4 is primarily expressed on antigen-presenting cells and can play a role in T-cell activation and help sustain an ongoing immune response (23), as well as serve to mediate the engulfment of apoptotic cells (24), thereby maintaining tolerance and preventing inflammation and autoimmunity against intracellular antigens released from the dying cells (25). By contrast, the one immune gene up-regulated in comparison 4, hCG40889 (complement factor H), is secreted in the plasma protein to regulate complement-mediated immunity, which plays a key role in microbial killing. By preventing excessive activation of the complement cascade, it participates in protecting host cells and tissues (26, 27).

We also identified six genes with auxiliary immune function, all of which were down-regulated in the infected Arizona vs. Alabama populations. We know that MG is exposed to host reactive oxygen species (ROS) (28) and that the generation of ROS by phagocytic cells during oxidative bursts is an important antibacterial mechanism (29). ROS are free radicals (e.g., superoxide  $O_2^-$ , hydroxyl radicals OH, hydrogen peroxide  $H_2O_2$ ) that are produced at high levels to kill internalized pathogens (30). Squalene epoxidase catalyzes the first oxygenation reaction of cholesterol biosynthesis (31) and has been suggested to play a role in the production of ROS, possibly via the effects of sterols on the localization of NADPH oxidase (32).

The action of ROS is nonspecific, and so as they accumulate, they damage host tissues and pathogens indiscriminately, e.g., by inducing DNA or cell damage through lipid peroxidation (33, 34). To minimize such costs, hosts have developed ROS-scavenging mechanisms, such as the enzyme superoxide dismutase, which catalyzes the dismutation of superoxide ( $O_2^-$ ) into oxygen ( $O_2$ ) and hydrogen peroxide ( $H_2O_2$ ). Thioredoxin, an oxidoreductase system induced by oxidative stress, has important antioxidant activities (35), and both ROS and thioredoxin can also influence downstream immune functions through the regulation of transcription factors and cytokines (36, 37). Spermidine/spermine N1-acetyltransferase is one of the main enzymes responsible for the regulation of intracellular polyamine (38). This protein can

be induced by the proinflammatory cytokine, tumor necrosis factor- $\alpha$ , to help maintain normal cellular physiology under inflammatory stress (39). Both spermine and spermidine exert protective functions of the cell under oxidative stress (40).

Rho GTPase is involved in several signal transduction pathways and plays an important role in the regulation and coordination of the innate immune response (reviewed in refs. 41 and 42). Rho GTPase proteins are involved in Toll-like receptor signaling, a key line of defense against microbial pathogens (43). They also form a subunit of the NADPH-oxidase complex where they regulate the formation of ROS during oxidative bursts (44). Another important role of Rho GTPase proteins is their implication in actin and microtubule regulation and cytoskeletal rearrangements mediating leukocyte chemotaxis and motility, phagocytosis, and lymphocyte cytotoxicity (45–47). The higher expression of cytoskeletal elements in infected birds from Alabama compared with infected birds from Arizona is consistent with the up-regulation of Rho GTPase in infected Alabama birds. Indeed,  $\beta$ -actin is one of the two isoforms present in the cytoplasm, and actin polymerization and depolymerization may be driven by actin-related protein and destrin (48).

Lymphocyte cytosolic protein (L-plastin) has been shown to stabilize actin filaments during T-lymphocyte migration (49), whereas the interaction between actin filaments and myosin and the phosphorylation of myosin regulatory light chains generate the contractile force necessary for cell migration (50).

Ubiquitin C targets cellular proteins for degradation in the proteasome (51). Ubiquitination, however, can also be reversible and play a role in the activity and localization of proteins in signaling pathways, as well as in the initiation of an immune response (for a review see ref. 52). The involvement of ubiquitin in immunity may be mediated through the specific degradation of inflammatory inhibitors (53); through the regulation of the tumor-necrosis factor receptor-associated factor 6, important in Toll-like receptor signaling (54); through the endocytosis of antibody-antigen complexes by Fc receptors (55, 56); or even through the generation of antigenic peptides important in MHC signaling (57).

- Luttrell MP, Stallknecht DE, Fischer JR, Sewell CT, Kleven SH (1998) Natural *Mycoplasma gallisepticum* infection in a captive flock of house finches. *J Wildl Dis* 34: 289–296.
- Roberts SR, Nolan PM, Hill GE (2001) Characterization of *Mycoplasma gallisepticum* infection in captive house finches (*Carpodacus mexicanus*) in 1998. *Avian Dis* 45: 70–75.
- Whitcomb RF (1983) Culture media for spiroplasmas. *Methods in Mycoplasmaology*, eds Razin S, Tully JG (Academic Press, New York), Vol 1, pp 147–158.
- Grodio JL, Dhondt KV, O'Connell PH, Schat KA (2008) Detection and quantification of *Mycoplasma gallisepticum* genome load in conjunctival samples of experimentally infected house finches (*Carpodacus mexicanus*) using real-time polymerase chain reaction. *Avian Pathol* 37:385–391.
- Wang Z, Farmer K, Hill GE, Edwards SV (2006) A cDNA microarray approach to parasite-induced gene expression changes in a songbird host: Genetic response of house finches to experimental infection by *Mycoplasma gallisepticum*. *Mol Ecol* 15: 1263–1273.
- van Bakel H, Holstege FCP (2004) In control: Systematic assessment of microarray performance. *EMBO Rep* 5:964–969.
- Hommais F, Pereira S, Acquaviva C, Escobar-Páramo P, Denamur E (2005) Single-nucleotide polymorphism phylotyping of *Escherichia coli*. *Appl Environ Microbiol* 71: 4784–4792.
- Noller AC, et al. (2003) Multilocus sequence typing reveals a lack of diversity among *Escherichia coli* O157:H7 isolates that are distinct by pulsed-field gel electrophoresis. *J Clin Microbiol* 41:675–679.
- Mebius RE, Kraal G (2005) Structure and function of the spleen. *Nat Rev Immunol* 5: 606–616.
- Davison F, Kaspers B, Schat K (2008) *Avian Immunology* (Elsevier, London), p 496.
- Borek F (1986) Previously unrecognized functions of the spleen: Development and maintenance of immune competence and regulation. *Crit Rev Immunol* 6:287–293.
- Brendolan A, Rosado MM, Carsetti R, Selleri L, Dear TN (2007) Development and function of the mammalian spleen. *Bioessays* 29:166–177.
- Smyth GK (2004) Linear models and empirical bayes methods for assessing differential expression in microarray experiments. *Stat Appl Genet Mol Biol* 3:e3.
- Hembruff SL, Villeneuve DJ, Parisenti AM (2005) The optimization of quantitative reverse transcription PCR for verification of cDNA microarray data. *Anal Biochem* 345: 237–249.
- Zar JH (2007) *Biostatistical Analysis* (Prentice Hall, Upper Saddle River, NJ).
- Bertolino P, Rabourdin-Combe C (1996) The MHC class II-associated invariant chain: A molecule with multiple roles in MHC class II biosynthesis and antigen presentation to CD4+ T cells. *Crit Rev Immunol* 16:359–379.
- Rubinstein N, Illarregui JM, Toscano MA, Rabinovich GA (2004) The role of galectins in the initiation, amplification and resolution of the inflammatory response. *Tissue Antigens* 64:1–12.
- Liu FT (2005) Regulatory roles of galectins in the immune response. *Int Arch Allergy Immunol* 136:385–400.
- Loser K, et al. (2007) Galectin-2 suppresses contact allergy by inducing apoptosis in activated CD8+T cells. *J Immunol* 182:5419–5429.
- Brown JA, et al. (2003) Blockade of programmed death-1 ligands on dendritic cells enhances T cell activation and cytokine production. *J Immunol* 170:1257–1266.
- Greenwald RJ, Freeman GJ, Sharpe AH (2005) The B7 family revisited. *Annu Rev Immunol* 23:515–548.
- Matute JD, et al. (2009) A new genetic subgroup of chronic granulomatous disease with autosomal recessive mutations in p40 phox and selective defects in neutrophil NADPH oxidase activity. *Blood* 114:3309–3315.
- Rodríguez-Manzanet R, DeKruyff R, Kuchroo VK, Umetsu DT (2009) The costimulatory role of TIM molecules. *Immunol Rev* 229:259–270.
- Kobayashi N, et al. (2007) TIM-1 and TIM-4 glycoproteins bind phosphatidylserine and mediate uptake of apoptotic cells. *Immunity* 27:927–940.
- Savill J, Fadok V (2000) Corpse clearance defines the meaning of cell death. *Nature* 407:784–788.
- Boon CJF, et al. (2009) The spectrum of phenotypes caused by variants in the CFH gene. *Mol Immunol* 46:1573–1594.
- de Córdoba SR, de Jorge EG (2008) Translational mini-review series on complement factor H: Genetics and disease associations of human complement factor H. *Clin Exp Immunol* 151:1–13.
- Jenkins C, Samudrala R, Geary SJ, Djordjevic SP (2008) Structural and functional characterization of an organic hydroperoxide resistance protein from *Mycoplasma gallisepticum*. *J Bacteriol* 190:2206–2216.
- Fang FC (2004) Antimicrobial reactive oxygen and nitrogen species: Concepts and controversies. *Nat Rev Microbiol* 2:820–832.
- Swindle EJ, Metcalfe DD (2007) The role of reactive oxygen species and nitric oxide in most cell-dependent inflammatory processes. *Immunol Rev* 217:186–205.

31. Abe I, et al. (2000) Green tea polyphenols: Novel and potent inhibitors of squalene epoxidase. *Biochem Biophys Res Commun* 268:767–771.
32. Posé D, et al. (2009) Identification of the Arabidopsis dry2/sqe1-5 mutant reveals a central role for sterols in drought tolerance and regulation of reactive oxygen species. *Plant J* 59:63–76.
33. Dröge W (2002) Free radicals in the physiological control of cell function. *Physiol Rev* 82:47–95.
34. Valko M, et al. (2007) Free radicals and antioxidants in normal physiological functions and human disease. *Int J Biochem Cell Biol* 39:44–84.
35. Nordberg J, Arnér ESJ (2001) Reactive oxygen species, antioxidants, and the mammalian thioredoxin system. *Free Radic Biol Med* 31:1287–1312.
36. Bubici C, Papa S, Dean K, Franzoso G (2006) Mutual cross-talk between reactive oxygen species and nuclear factor-kappa B: Molecular basis and biological significance. *Oncogene* 25:6731–6748.
37. Sen CK, Packer L (1996) Antioxidant and redox regulation of gene transcription. *FASEB J* 10:709–720.
38. Casero RA, Jr, Pegg AE (1993) Spermidine/spermine N1-acetyltransferase: The turning point in polyamine metabolism. *FASEB J* 7:653–661.
39. Babbar N, Murray-Stewart T, Casero RA Jr (2007) Inflammation and polyamine catabolism: The good, the bad and the ugly. *Biochem Soc Trans* 35:300–304.
40. Rider JE, et al. (2007) Spermine and spermidine mediate protection against oxidative damage caused by hydrogen peroxide. *Amino Acids* 33:231–240.
41. Bokoch GM, Knaus UG (2003) NADPH oxidases: Not just for leukocytes anymore!. *Trends Biochem Sci* 28:502–508.
42. Scheele JS, Marks RE, Boss GR (2007) Signaling by small GTPases in the immune system. *Immunol Rev* 218:92–101.
43. Aderem A, Ulevitch RJ (2000) Toll-like receptors in the induction of the innate immune response. *Nature* 406:782–787.
44. Kao YY, Gianni D, Bohl B, Taylor RM, Bokoch GM (2008) Identification of a conserved Rac-binding site on NADPH oxidases supports a direct GTPase regulatory mechanism. *J Biol Chem* 283:12736–12746.
45. Cicchetti G, Allen PG, Glogauer M (2002) Chemotactic signaling pathways in neutrophils: From receptor to actin assembly. *Crit Rev Oral Biol Med* 13:220–228.
46. Khurana D, Leibson PJ (2003) Regulation of lymphocyte-mediated killing by GTP-binding proteins. *J Leukoc Biol* 73:333–338.
47. Scott CC, et al. (2005) Phosphatidylinositol-4,5-bisphosphate hydrolysis directs actin remodeling during phagocytosis. *J Cell Biol* 169:139–149.
48. Yeoh S, Pope B, Mannherz HG, Weeds A (2002) Determining the differences in actin binding by human ADF and cofilin. *J Mol Biol* 315:911–925.
49. Samstag Y, Eibert SM, Klemke M, Wabnitz GH (2003) Actin cytoskeletal dynamics in T lymphocyte activation and migration. *J Leukoc Biol* 73:30–48.
50. Mizutani T, Haga H, Koyama Y, Takahashi M, Kawabata K (2006) Diphosphorylation of the myosin regulatory light chain enhances the tension acting on stress fibers in fibroblasts. *J Cell Physiol* 209:726–731.
51. Varshavsky A (2003) The N-end rule and regulation of apoptosis. *Nat Cell Biol* 5:373–376.
52. Boyer L, Lemichez E (2004) Targeting of host-cell ubiquitin and ubiquitin-like pathways by bacterial factors. *Nat Rev Microbiol* 2:779–788.
53. Silverman N, Maniatis T (2001) NF-kappaB signaling pathways in mammalian and insect innate immunity. *Genes Dev* 15:2321–2342.
54. Deng L, et al. (2000) Activation of the IkkappaB kinase complex by TRAF6 requires a dimeric ubiquitin-conjugating enzyme complex and a unique polyubiquitin chain. *Cell* 103:351–361.
55. Booth JW, Kim MK, Jankowski A, Schreiber AD, Grinstein S (2002) Contrasting requirements for ubiquitylation during Fc receptor-mediated endocytosis and phagocytosis. *EMBO J* 21:251–258.
56. Yamakami M, Yoshimori T, Yokosawa H (2003) Tom1, a VHS domain-containing protein, interacts with tollip, ubiquitin, and clathrin. *J Biol Chem* 278:52865–52872.
57. Goldberg AL, Cascio P, Saric T, Rock KL (2002) The importance of the proteasome and subsequent proteolytic steps in the generation of antigenic peptides. *Mol Immunol* 39:147–164.

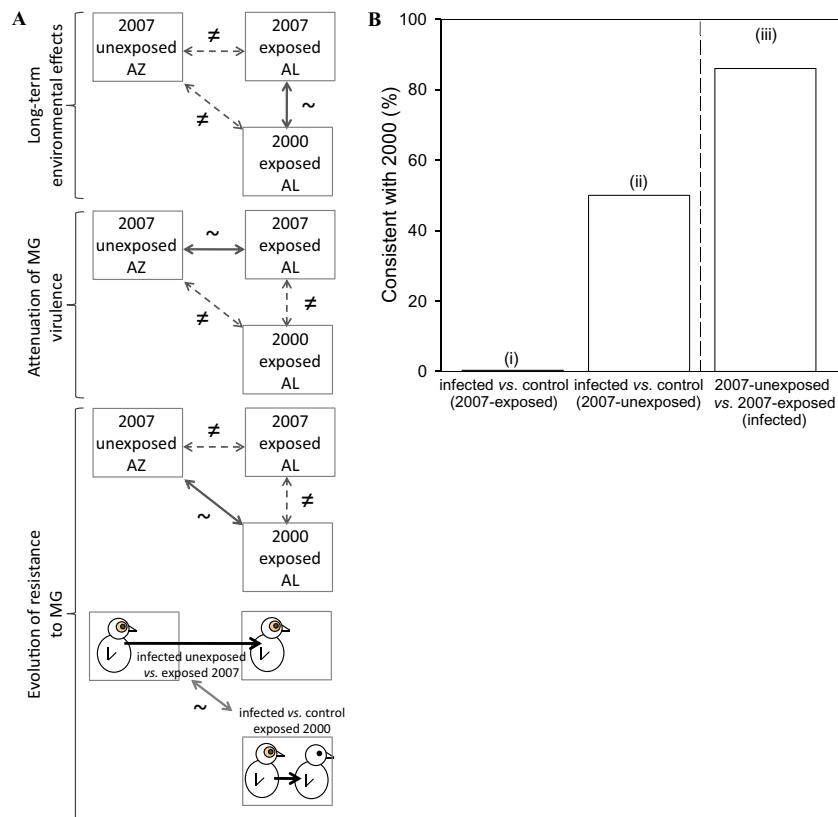


**Fig. S1.** Comparisons of expression profiles at different stages of the epizootic. (A) Hypotheses and predictions: long-term condition changes predicted that comparisons between infected and controls in Alabama in 2007 and in Alabama in 2000 would be more similar to each other than they would be to the comparison between infected and controls in Arizona in 2007; MG attenuation predicted that Alabama in 2007 and Arizona in 2007 would be more similar to each other than they would be to the populations Alabama in 2000; evolution of resistance to MG predicted that Arizona in 2007 and Alabama in 2000 would be more similar to each other than they would be to Alabama in 2007 and that the comparison infected Arizona vs. infected Alabama in 2007 would be similar to the comparison infected vs. controls in Alabama in 2000. Solid arrows indicate greater similarity and dotted arrows greater dissimilarity. (B) Of 14 expression differences found between infected and control birds from MG exposed-Alabama in 2000 (i.e., early in the epizootic) (1): (i) none was common to those found in the same comparison in the same population later in the epizootic (in 2007), despite birds being captured from an identical location 7 y apart; (ii) 6 birds were qualitatively identical to those found in the same comparison but from the MG unexposed-Arizona population in 2007, despite the two populations being isolated for at least 60 y; and (iii) 11 birds were qualitatively identical to differences found in infected birds between MG unexposed-Arizona and MG exposed-Alabama in 2007.

1. Wang Z, Farmer K, Hill GE, Edwards SV (2006) A cDNA microarray approach to parasite-induced gene expression changes in a songbird host: Genetic response of house finches to experimental infection by *Mycoplasma gallisepticum*. *Mol Ecol* 15:1263–1273.

**Table S1. Summary of the 52 genes found to be significantly differentially expressed in at least one of the four comparisons in the microarray and for which we identified a vertebrate homolog**

Vertebrate homolog	Accession no.	e-Value	Identity	Species	GO category	GO function
Predicted: T-cell Ig and mucin domain containing 4	XM_002194781.1	5.00E-132	304/326 (93%)	<i>Taeniopygia guttata</i>	Immune	Maintenance of immune response, engulfment of apoptotic cells
Putative MHC class II-associated invariant chain Ii*	DQ215319.1	3E-131	462/550 (84%)	<i>Taeniopygia guttata</i>	Immune	Role in assembly of MHC class II
Predicted: Lectin galactoside-binding soluble 2 protein*	XM_002196008.1	4E-170	371/392 (94%)	<i>Taeniopygia guttata</i>	Immune	Regulator of cellular immune function
Predicted: Programmed death ligand 1	XM_424812.2	3.00E-45	200/245 (81%)	<i>Gallus gallus</i>	Immune	B-Cell differentiation, regulation of T-cell activation
TCR $\beta$ -chain	AF068228.1	8E-72	284/347 (81%)	<i>Anas platyrhynchos</i>	Immune	T-cell recognition of foreign antigens
Putative Ig J	DQ213324.1	0	709/804 (88%)	<i>Taeniopygia guttata</i>	Immune	Antigen binding
Predicted: Neutrophil cytosolic factor 4 (40 kDa)	XM_002196200.1	4E-72	167/175 (95%)	<i>Taeniopygia guttata</i>	Immune	Component of the superoxide-producing phagocyte NADPH oxidase
Predicted: Ig superfamily member 4A isoform a	XM_417901.2	3E-84	242/273 (88%)	<i>Gallus gallus</i>	Immune	Positive regulator of cytokine secretion, activated T lymphocyte proliferation
Putative parathymosin variant 1*	DQ214395.1	3E-180	517/594 (87%)	<i>Taeniopygia guttata</i>	Immune	May block prothymosin, which confers resistance to opportunistic infections
Predicted: hCG40889 (complement factor H)	XM_002192303.1	7E-79	227/257 (88%)	<i>Taeniopygia guttata</i>	Regulation of immunity	Regulation of complement activation, restricting this innate defense mechanism to microbial infections
Thioredoxin	EF192008.1	0	550/592 (92%)	<i>Taeniopygia guttata</i>	Redox metabolism (auxiliary immune)	Antioxidant activity, regulation of oxidative stress-induced signal transduction
Spermidine/spermine N1-acetyl transferase	EF192029.1	2E-93	197/201 (98%)	<i>Taeniopygia guttata</i>	Polyamine catabolism (auxiliary immune)	Polyamine catabolism, response to inflammation
Predicted: Squalene epoxidase*	XM_002187235.1	4E-175	628/664 (94%)	<i>Taeniopygia guttata</i>	Redox metabolism (auxiliary immune)	Sterol biosynthesis, ROS production
Cytochrome c oxidase subunit I*	EF484222.1	0	755/837 (90%)	<i>Mimus gundlachi</i>	Redox metabolism	Mitochondrial respiratory chain complex IV
Cytochrome b	AY495387.1	0	376/376 (100%)	<i>Carpodacus erythrinus</i>	Redox metabolism	Mitochondrial respiratory chain complex III
Cytochrome c oxidase subunit II	EF484237.1	1E-56	153/167 (91%)	<i>Cinnyricinclus leucogaster</i>	Redox metabolism	Mitochondrial respiratory chain complex IV
NADH dehydrogenase subunit 4*	AY567938.1	0	639/773 (82%)	<i>Ciconia nigra</i>	Redox metabolism	Mitochondrial respiratory chain complex I
Cytochrome c oxidase subunit III*	DQ385208.1	3.00E-64	208/242 (85%)	<i>Pedionomus torquatus</i>	Redox metabolism	Mitochondrial respiratory chain complex IV
Cytochrome c oxidase subunit VIIa 2	DQ213599.2	0	444/459 (96%)	<i>Taeniopygia guttata</i>	Redox metabolism	Mitochondrial respiratory chain complex IV
Ubiquitin C*	DQ216247.1	0	639/691 (92%)	<i>Taeniopygia guttata</i>	Proteolysis (auxiliary immune)	Protein degradation
Predicted: Nedd4 family interacting protein 1	XM_002193395.1	0	390/399 (97%)	<i>Taeniopygia guttata</i>	Proteolysis	Ubiquitin-mediated proteolysis
Prosaposin variant 3	DQ214627.1	5E-59	168/187 (89%)	<i>Taeniopygia guttata</i>	Metabolism	Lipid metabolism and transport
Predicted: Phospholipase D family, member 4	XM_002200327.1	7.00E-86	Haut du formulaire 219/239 (91%)	<i>Taeniopygia guttata</i>	Metabolism, lipid catabolism	Hydrolase and phospholipase activity
N-acetyltransferase 5	XM_002189727.1	6E-70	162/169 (95%)	<i>Taeniopygia guttata</i>	Metabolism	Acytransferase and N-acetyltransferase activity
Predicted: RhoA GTPase	XM_002196158.1	0	546/558 (97%)	<i>Taeniopygia guttata</i>	Oxidative burst, signal transduction (auxiliary immune)	GTPase activity, subunit of NADPH oxidase, Rho protein signal transduction, motility of phagocytic cells
MLTK- $\beta$ (predicted: sterile $\alpha$ -motif and leucine zipper containing kinase AZK)	XM_002198892.1	0	770/786 (97%)	<i>Taeniopygia guttata</i>	Signal transduction, proapoptosis, response to stress	Protein phosphorylation
Predicted: MAK-like kinase (ICK)	XM_002195712.1	0	478/488 (97%)	<i>Taeniopygia guttata</i>	Signal transduction	Protein phosphorylation

**Table S1. Cont.**

Vertebrate homolog	Accession no.	e-Value	Identity	Species	GO category	GO function
Tyrosine 3-monooxygenase/tryptophan 5-monooxygenase activation protein (YWHAQ)	NM_001006415.1	1E-164	409/451 (90%)	<i>Gallus gallus</i>	Signal transduction	Protein scaffolding
Predicted: Pleckstrin homology domain	XM_002189748.1	6E-166	346/359 (96%)	<i>Taeniopygia guttata</i>	Signal transduction	Binds inositol phosphates
Predicted: Protein 4.1-G	XM_001232112.1	0	830/962 (86%)	<i>Gallus gallus</i>	Immune, cytoskeleton	T-cell activation processes
Cytoplasmic $\beta$ -actin	X00182.1	1E-48	144/159 (90%)	<i>Gallus gallus</i>	Cytoskeleton	Cell motility and structure
Predicted: Lymphocyte cytosolic protein*	XM_002198488.1	8.00E-125	266/276 (96%)	<i>Taeniopygia guttata</i>	Cytoskeleton (auxiliary immune)	Actin-binding protein in hemopoietic cell lineages
Destrin (DSTN)	NM_205528.1	5E-117	282/303 (93%)	<i>Gallus gallus</i>	Cytoskeleton	Actin-depolymerizing protein
Actin-related protein 3 (ARP3)	AF498322.1	2E-86	304/361 (84%)	<i>Gallus gallus</i>	Cytoskeleton	Actin polymerization
Predicted: Myosin regulatory light chain	XM_002186983.1	3E-150	312/322 (96%)	<i>Taeniopygia guttata</i>	Cytoskeleton	Regulator of myosin
Predicted: Heat-shock protein 90a*	X07265.1	4E-130	310/337 (91%)	<i>Gallus gallus</i>	Stress	Molecular chaperone
Nuclear ribonucleoprotein A/B (HNRNPAB)	NM_205328.4	1E-132	301/320 (94%)	<i>Gallus gallus</i>	Transcription	Positive regulation of transcription
Mediator complex subunit SOH1	EF191826.1	0	418/432 (96%)	<i>Taeniopygia guttata</i>	Transcription	RNA polymerase II transcription mediator activity, mediates activation of stress-responsive kinases
Translation initiation factor EIF4G2 variant 1	NM_001099860.1	0	608/657 (92%)	<i>Gallus gallus</i>	Translation	regulation of translational initiation
Translation elongation factor 1 $\alpha$ 1*	NM_204157.2	5E-116	244/250 (97%)	<i>Gallus gallus</i>	Translation	Translation elongation
40S ribosomal protein S20	DQ217356.1	4E-52	130/137 (94%)	<i>Taeniopygia guttata</i>	Translation	Component of the 40S subunit of the ribosome
Putative ribosomal protein S15	DQ213656.1	2E-50	126/132 (95%)	<i>Taeniopygia guttata</i>	Translation	Component of the 40S subunit of the ribosome
Predicted: Splicing factor 3b, subunit 3 (130 kDa)	XM_002188348.1	3E-102	215/220 (97%)	<i>Taeniopygia guttata</i>	Nucleic acid and protein binding	mRNA processing, protein complex assembly, RNA splicing
Nucleic acid binding protein RY-1 variant 3	DQ216570.1	0	495/508 (97%)	<i>Taeniopygia guttata</i>	Nucleic acid binding	RNA splicing
Ribosomal protein large P2	DQ213409.2	3E-92	202/209 (96%)	<i>Taeniopygia guttata</i>	Translation	Translation elongation
Predicted: DEAD/H (Asp-Glu-Ala-Asp/His) box polypeptide 3	XM_002190542.1	0	383/385 (99%)	<i>Taeniopygia guttata</i>	Translation	RNA helicase, Translation initiation
Predicted: ribosomal protein S24*	XM_002195573.1	1E-117	254/264 (96%)	<i>Taeniopygia guttata</i>	Translation	Translation initiation
Eukaryotic translation initiation factor eIF4E*	DQ213184.1	0	818/831 (98%)	<i>Taeniopygia guttata</i>	Translation	Regulation of translational initiation
Predicted: SEC61 $\gamma$ -subunit	XM_002198448.1	2E-55	192/197 (97%)	<i>Taeniopygia guttata</i>	Transport	Intracellular protein transmembrane transport
Putative hemoglobin $\alpha$ *	DQ216727.1	1E-132	315/342 (92%)	<i>Taeniopygia guttata</i>	Oxygen transport	
Predicted: dyslexia susceptibility 1 candidate 1	XM_002197669.1	8E-79	185/195 (94%)	<i>Taeniopygia guttata</i>	Binding	
Predicted: Epidermal differentiation-specific protein	XM_002192313.1	7E-83	199/213 (93%)	<i>Taeniopygia guttata</i>	Cell differentiation	

We indicate the Gene Ontology category and function; many genes were implicated in several biological processes and we favored the processes associated with immune functioning or stress response. Gene Ontology category and function were determined using Harvester (<http://harvester.fzk.de/harvester/>). Note that functions were mostly determined from studies on humans and mice; therefore, although they are likely to be conserved, we cannot rule out that proteins have evolved to serve different roles in house finches. Genes with an identified auxiliary immune function are indicated as such in parentheses.

\*Genes that are also differentially expressed in the macroarray experiment (1); two new genes were identified with updated BLAST searches (parathymosin, eukaryotic translation initiation factor eIF4E).

1. Wang Z, Farmer K, Hill GE, Edwards SV (2006) A cDNA macroarray approach to parasite-induced gene expression changes in a songbird host: Genetic response of house finches to experimental infection by *Mycoplasma gallisepticum*. *Mol Ecol* 15:1263–1273.